

# FE-MODELING OF DYNAMIC EXPERIMENTAL TESTING WITH LARGE ELASTIC-PLASTIC DEFORMATIONS

Patrik Canmo and Henrik Snygg

Department of Mechanics  
SP Swedish National Testing and Research Institute  
SE-501 15 Boras  
SWEDEN

## ABSTRACT

Several types of dynamic tests are carried out at SP Swedish National Testing and Research Institute. The tests considered in this paper, which are all simulated with FE-calculations, are as follows: a drop test of cask filled with water, a tennis racket/ball test, a test of a full face protector for hockey players and an impact test of a simplified bumper. To obtain a high-quality verification of the FE-results high-speed video recording of the test sequence is done in all four cases. Parameter studies are done regarding velocity and drop height. The FE-models are built up in the commercial software ABAQUS and I-deas, and are all solved numerically with ABAQUS/Explicit<sup>[1]</sup>. The material models used in the FE-calculations include linear elastic, elastic-plastic with non-linear hardening, hyperelastic and linear hydrodynamic behavior. Different types of tests are carried out on material specimens in order to determine the material parameters used in the FE-models.

## NOMENCLATURE

$E$	Young's modulus of elasticity
$G$	Shear modulus of elasticity
$\nu$	Poisson's ratio
$K$	Bulk modulus
$\rho_0$	Density
$c_0$	Wave speed
$\sigma_{0.2}$	Offset yield stress
$\sigma_Y$	Yield stress

## 1 INTRODUCTION

Several different types of tests, are regularly performed at SP's Mechanical laboratory which include large deformations during very short time or transient loading, for example drop test, crash test, helmet test and bursting test. There is an

increasing interest to solve these events by finite element calculation and SP's close relation between FE-calculation and laboratory resources guaranties unique possibilities for calculation, simulation and verification.

The objective with this project was to improve the skills in FE-calculation and to offer a complement to the experimental testing. A parametric study can easily be done in a FE-calculation after the results are verified. What will happen if we change the thickness, change material or improve the design? To answer such questions by experimental tests alone can be a very time consuming and resource demanding venture. Moreover, depending on the design changes in question the tests may not always render visible results. A more fruitful strategy to answer these questions and to obtain a larger comprehension of the dynamic behavior of the product is to combine experimental tests with finite element analyses.

Documentation of fast dynamic events was done by video recording with a high-speed video camera. This can be used to verify explicit FE-results of dynamic events with large elastic-plastic deformations. The high-speed video camera can take 1000 pictures per second with an exposure time of 0.1 to 1 ms. The system includes an analysis program where it is possible to measure the movement or displacement of the object via distance points on the object. With the high-speed video camera and a wide range of sensors, most types of FE-verifications from a simple stress strain analysis to a complex explicit analysis, can be covered.

## 2 DROP TEST

The first test to evaluate in this paper is the results from a standard drop test method<sup>[2]</sup>, carried out frequently at the Division of Transport Safety. Explicit finite element calculations are performed and the results are verified against the experimental results for the same test configuration as in the experimental test. The test configuration comprises a cask partially

filled with water, dropped onto a rigid plate.

## 2.1 Test set up

The drop procedure was carried out with 3 tests at a drop height of 1m and 1 test at a drop height of 2m. Each cask was released with its center of gravity vertically over the point of impact corresponding to an inclination of 32 degrees. The target was a rigid, non-resilient, flat and horizontal plate connected to the primary rocks. For the tests the casks were partially filled with water to 90 percent of the casks capacity, which gave a total weight of 24 kg.

All four tests were shot with the high-speed video camera, which gave a clear picture of the deformation history of the cask. No material tests were done for this test. The general hydrodynamic material properties for the water were taken from<sup>[1]</sup> and the elastic-plastic material properties for the cask were given by the manufacturer.

## 2.2 FE-model

The FE-model of the cask and the water was built up in I-deas with shell and solid-elements and exported to ABAQUS where the calculation and post processing were performed. The deformed model geometry without the water is shown in Figure 1. By using symmetry only half of the cask and water were modeled. All material and contact definitions were defined in ABAQUS.



Figure 1: FE-model showing half of the deformed cask (from the inside), dropped from a height of 2m.

A Newtonian viscous shear model and a linear equation of state were used to model the water. The bulk modulus of water was chosen to  $K = 2.07$  MPa which corresponds to a wave speed of  $c_0 = 45.85$  m/s, see equation 1.

$$c_0 = \sqrt{K/\rho_0} \quad (1)$$



Figure 2: Picture of the impact taken from the video recording, drop height of 2m.

Since water is almost an inviscid fluid only a small shear viscosity was used to avoid the mesh to tangle. The shear viscosity and the density of the water was chosen as  $13 \cdot 10^{-4}$  1/sec and  $\rho_0 = 980$  kg/m<sup>3</sup> respectively. The material properties for the cask was according to the manufacturer  $E = 206$  GPa and  $\sigma_{0.2} = 550$  MPa.

Contact conditions were defined between the rigid plate and the outside of the cask and between the outside surface of the water and the inside of the cask. The shell thickness of the cask was not taken into account when modeling the water. Instead, enforced contact between the outer surface of the water and the mid-surface of the shell was used. A pure master-slave contact condition has been used to model the contact between the solids and the shells. Depending on the much stiffer cask compared to the water the shells are defined as masters and not the solids as in normal cases. Friction is also specified between the rigid plate and the cask with a coefficient of friction of 0.1. Due to buckling of the wall at the impact point, self-contact was defined for all the shell elements of the lower part of the cask.

Instead of using the actual drop height the cask was modeled just above the rigid plate with an initial impact velocity corresponding to respective drop height. The calculated impact velocities for the drop heights 1 m and 2 m were 4.43 m/s and 6.26 m/s, respectively.

## 2.3 Results

A calculation time of 5 ms was enough to model the whole sequence from the impact to the cask has deformed and started to tilt. In a visual comparison between the FE-calculation and the experimental result, a good agreement can be seen. The buckling along the bottom circumference that can be seen in

the video is also appearing in the calculation. The number of buckles is identical, and the size and shape are qualitatively the same. The deformed cask and the buckling of the bottom circumference are shown in Figure 1 (without water). Verification of the drop height of 1 m shows a 50 mm deformation of the impact point in the video compared to 45 mm for the FE-calculation. The upper part of the cask is not affected by the impact.

Increasing the drop height to 2 m affected only the deformation at the impact point. The deformation increased with approximately 50 % to 60 mm which correspond very well with the experimental results, see Figure 2. The buckling along the bottom circumference was qualitatively unchanged when increasing the drop height.

### 3 FULL FACE PROTECTOR TEST

Head protectors for ice hockey players comprise helmets and, in some cases, an associated full face protector. At SP, these are tested according to a European standard<sup>[3]</sup>, where a full face protector is always tested and assessed together with the helmet for which it is intended. However, here we focus on the full face protector as a separate unit and no intentions to model the helmet or the interaction between helmet and face protector are made.

#### 3.1 Test set up

The test set up used here was simplified as compared to the standard set up. The rear ends of the face protector were fixed to a rigid plate instead of being fixed to a helmet placed on a head form. The test procedure can be described as follows: A puck accelerator (puck cannon) gives the hockey puck a specific velocity, which is variable between 10 m/s and 36 m/s. The equipment for measuring and recording the velocity has a limit of error of 2%. At the front of the accelerator a guiding device gives the puck the desired direction. This device can be replaced to fit other objects than a puck, e.g. a tennis ball (see Section 4). The motion of the puck is thereby controlled and follows a straight line to the point of impact.

#### 3.2 Numerical analyses

To analyze the effect of the puck hitting the face protector, a series of finite element analyses were performed. The (deformed) finite element mesh of the puck and the face protector is shown in Figure 3. The puck is built up of 4-node solid linear tetrahedrons and the face protector consists of 2-node linear beam elements with a radius of 1.4 mm.

Material tests were carried out to determine the material data for the puck and the face protector, respectively. The tension test of the steel, which the face protector was made of, gave

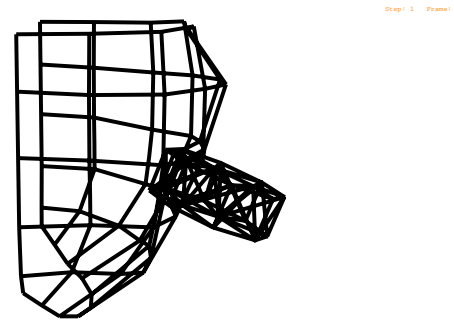


Figure 3: FE-model showing the deformed face protector during impact of the puck (velocity=31 m/s).

the following result:  $E = 220$  GPa and  $\sigma_{0.2} = 600$  MPa. The peak stress was only slightly higher than  $\sigma_{0.2}$  so the material was modeled as elastic-perfectly plastic. The puck was modeled as elastic, and a compression test gave  $E = 62$  MPa. Contact conditions were defined between the puck and the face protector.



Figure 4: Maximum deformation of the face protector during impact of the puck (velocity=31 m/s) .

#### 3.3 Results

Three tests were carried out with the puck velocities 32 m/s, 31 m/s and 28 m/s, respectively. The deformations of the face protector were similar in the three cases. All tests were recorded by the high-speed video camera.

In Figure 4 we can observe the maximum deformation of the face protector during experimental impact of the puck. In this case, the velocity was measured to 31 m/s, the maximum deformation was measured to 40 mm and the remaining deformation, after impact, to 25 mm. No cracking or breakage in the joints of the bars could be observed.

In the FE-calculations, the initial velocity of the puck was set equal to the velocity measured in the experimental test. The maximum deformation during impact, which are shown in Figure 3, was 38 mm (velocity=31 m/s). At this point, the maximum stress 600 MPa was reached in several of the beam elements, but when the puck bounced back the stresses were relaxed. After the impact, the remaining deformation was measured to 20 mm. No special modeling of the joints was made, they were considered to have the same properties as the beam elements. Since no breakage of joints was observed in the experiments, this is an acceptable simplification.

#### 4 TENNIS RACKET/BALL TEST

In this section we verify and evaluate the results from an explicit finite element calculation on a tennis ball hitting a tennis racket. A parametric study regarding the ball's impact velocity was done. Experimental tests have been performed on both the ball and of the impact of the ball hitting the racket to verify the FE-calculation. Several tests were done to obtain material properties of the different materials used in the test configurations.

##### 4.1 Test set up

As a pre-test, the tennis ball was shot against a concrete wall to calibrate the material behavior of the ball. The same puck accelerator (puck cannon) used in the previous section is also used for the tests in this section. Four different velocities in the range of 12.0 m/s to 42.4 m/s were used to calibrate the ball. Figure 5 shows the maximum deformed state of the ball just before leaving the wall. The impact velocity of the ball was 42.4 m/s.



Figure 5: High-speed video showing the maximum deformed state of the tennis ball (velocity=42.4 m/s).

The experimental test set up for the racket can be seen in Figure 6, the picture shows the racket placed in front of the puck cannon and where the ball is shoot a little bit eccentric onto the strings. The corrugated cardboard with the black and white adhesive tape that can be seen behind the racket in the picture, is used to measure the deflection of the frame during the impact. The handle of the racket was clamped at the middle.



Figure 6: Test set up showing the tennis-ball hitting the strings of the tennis-racket.

##### 4.2 Material test

Material property tests have been done for the racket frame, the strings and the tennis ball. Three simple tension tests were done for the strings where the initial mean Young's modulus was determined to be 2.5 GPa.

The tennis ball, which is assumed to be made of hyperelastic rubber, was tested with both hysteresis tensile tests and hysteresis compression tests. Four test specimens were tested with hysteresis uniaxial tensile test according to the international standard<sup>[4]</sup>. The test was carried out with 4 cycles at a 250 mm/min rate of traverse, extended to 50 %, then immediately returned. The compression tests were carried out in the same manner as the tensile tests, but with a 50 mm/min rate of traverse. Figure 7 shows the hysteresis results for the first test specimen. From the test results the mean values of the hyperelastic material properties were calculated and used in the FE-model of the tennis ball.

The orthotropic engineering material constants for a plane stress material of a similar racket frame were given by the manufacturer. By combining the results from a three point bending test with the given relationships between the two orthogonal material directions, valid material properties for the frame material were obtained. The three point bending test was performed by applying a load at the middle of a sim-

ply supported specimen, taken from the tested racket. The load was then gradually increased and the middle deflection was measured until break was achieved. From the measured load-deflection curve an actual Young's modulus was calculated and the determined orthotropic engineering constants for the frame were derived as follows:

$$E_x = 30.0 \text{ GPa} \quad E_y = 4.28 \text{ GPa} \quad G_{xy} = 7.68 \text{ GPa}$$

$$\nu_{xy} = 1.2 \quad \nu_{yx} = 0.15$$

Where x defines the direction parallel with the racket and y is the direction perpendicular to the racket.

### 4.3 FE-model

The tennis ball used in the test consists of rubber core, cord and a layer of felt. However, only the rubber core was modeled in the FE-calculation. The rubber core was modeled with shell elements in IDEAS and exported and positioned in ABAQUS. By combining the uniaxial tensile and compression tests a good starting point for the hyperelastic material behavior was achieved, see Figure 7.

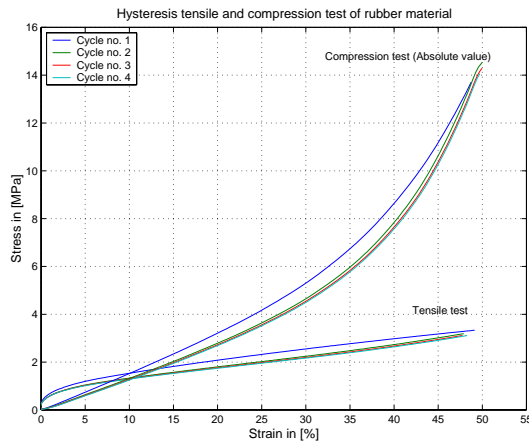


Figure 7: Figure showing the 4 cycles of the tensile and compression test of the rubber.

Calibration of the material properties was necessary, due to the omission of felt and the cord. The material behavior was obtained by calibrating the measured material properties by shooting the ball against the concrete wall and then compare the FE-result with the experimental results visually. A range of speed from 12 m/s to 42 m/s was used to get a good visual characterization of the hyperelastic material behavior.

To model the elliptic cross section of the racket frame a simplified plain cross section was used. The width of the simplified cross section was set equal to that of the actual cross section. The height was chosen by imposing the condition that the plane cross section should have the same moment of inertia as the elliptic cross section. This is an adequate repre-



Figure 8: FE-model showing the tennis-ball hitting the strings of the tennis-racket.

sentation of the frame, since bending and deflection are the dominating features of interest in this study. The derived engineering constants specified above were used to model the orthotropic material behavior of the frame. No damping effect was modeled in the frame.

The strings were modeled in ABAQUS with truss elements connected to each other at every overlapping section and where the end nodes of each string were connected to the midsurface of the frame shells. A linear elastic material model was used to model the material behavior of the strings with the measured Young's modulus defined above. The strings were modeled with an initial stress of 201 MPa, corresponding to a measured initial load of 267 N.

Clamped boundary conditions were applied to the middle of the handle to constrain all six degrees of freedom. The ball was positioned very close to the strings and slightly eccentric with an initial velocity corresponding to the velocity used in the experimental test.

### 4.4 Results

A typical hyperelastic material behavior of the ball can clearly be seen in the video after the tennis ball has left the wall. A stabilization of the sinusoidal deformation on the way back from the wall to its original state takes place first after 5 to 6 oscillations. The first test calculations of bouncing tennis balls showed that the FE-model was not able to capture the proper dynamic behavior. Due to the omission of felt and core and the use of hyperelastic material properties obtained from quasi-static test results the model of the ball appeared to be too soft. Increasing the stiffness in the FE-calculations with a factor of three showed that the deformation of the ball correlated better with the experimental results for all velocities in the tested range. This was done by a visual comparison of the FE-results and the experimental results.

\*) The turning back of the racket frame was not recorded

Ball speed	25.1 m/s		32.5 m/s	
	pos. dir.	neg. dir.	pos. dir.	neg. dir.
Experimental	56 mm	50 mm	82 mm	— *)
FE-model	51 mm	49 mm	68 mm	63 mm
Accuracy	9 %	2 %	17 %	—

**TABLE 1: A summary of the results from the deflection of the frame at the impact point.**

Verification of the FE-results for the racket and the ball can be performed in various way, either by measuring the deflection of the frame at the level of the impact point or by visually comparing the behavior of the racket and the ball during the animation of the FE-results and the high-speed video recording. The verification of the frame deflection of the FE-model, see Figure 8, corresponds well with the experimental results for the lower speed but less well for the higher speed, see Table 1. The accuracy in the visually sampled values given in the Table are  $\pm 2$ mm. The deviation from the experimental results especially for the higher speed could be explained by the simplified cross section used for the frame.

The dynamic deflection of the racket was at the beginning of the impact very low until the ball left the strings, which can be seen in Figure 6. The picture is taken from the high-speed video recording showing that the ball and the strings absorb all the energy in the beginning of the impact. Then after the ball has left the strings a large deflection of the racket begins. A deflection of 56 mm is measured at the turning point, for a velocity of 25.1 m/s, then the direction of speed reverse and nearly achieve the same deflection on the the turning back. This behavior is obtained in both the experimental test and in the FE-result. Moreover, the same stabilization of the sinusoidal deformation behavior of the ball, after leaving the strings, can be seen in both the experimental test and the FE-result.

## 5 IMPACT TEST OF A SIMPLIFIED BUMPER

The last test in this paper is devoted to the impact of a rigid wall into a simplified bumper. The test was carried out on a crash test lane, on which a sledge can be accelerated to the desired velocity (up to 20 m/s). It is used mostly for crash testing of vehicle components, such as safety belts, interior fittings, car seats, liquid fuel tanks, windcreens and child restraint systems.

### 5.1 Test set up

The simplified bumper was constructed by quadratic beams of steel with the dimensions 40x40 mm and a wall thickness of 4 mm, see Figure 9. The length of the front beam was 800mm

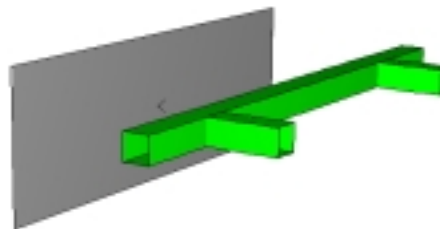


**Figure 9: Test set up of the rigid wall and the simplified bumper.**

and the support beams were 110mm. These three parts were welded together. The support beams were then clamped to a rigid plate at the end of the lane and the rigid wall, which had a width of 600mm, was attached to the sledge and placed so that the center of the wall (marked with an x in Figure 9) would hit the right support beam.

### 5.2 FE-model

The FE-model of the bumper was built up of 4-node shell elements, whereas the wall was modelled as a rigid body. The bumper was modelled as elastic-plastic with linear isotropic hardening with the following data:  $E = 206$  GPa,  $\sigma_Y = 270$  MPa and a peak stress of 440 MPa at 25% plastic strain. The rigid wall and the front of the bumper were defined as contact surfaces, where the rigid wall was the master surface. The coefficient of friction was set to 0.3. In Figure 10 the (deformed) FE-model of the bumper is shown.

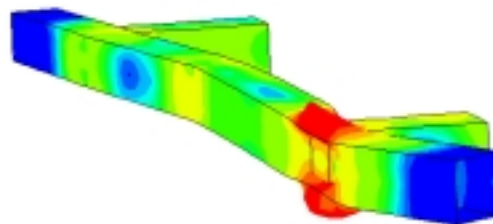


**Figure 10: The von Mises stress at maximum deformation of the bumper.**

### 5.3 Results

At the experimental test, the velocity of the sledge was measured to 2.8 m/s and the total mass of the wall and the sledge was 1500 kg. The impact was recorded by the high-speed camera and the maximum deformation of the bumper is shown in Figure 11. A large plastic deformation of the front beam can be observed in front of the right support beam. However, no breakage or cracks were observed, neither in the beams nor in the welds. This means that the elastic-plastic model used in the FE-calculations should be sufficient.

The result of the FE-calculation is shown in Figure 10, where the von Mises stress distribution is plotted at maximum deformation. As expected, the peak stress of 360 MPa was reached in the front beam in front of the right support beam.

A comparison of the experimental results and the FE-results gave a good agreement. The deformations are of the same magnitude and differ no more than 10% at any place.



Figure 11: High-speed video recording of the deformation of the bumper during impact.

## 6 CONCLUSIONS

Four different types of dynamic tests have been investigated in this paper. All tests have been recorded by a high-speed video camera and simulated numerically by a series of dynamic finite element analyses. Generally, the FE-results were within good agreement with the high-speed video recordings and the final state of deformation for all four tests.

The concept of using the high-speed video camera for verification of the FE-results and for calibrating material parameters has been an invaluable tool. One problem, which was solved by using this technique, was to calibrate the hyperelastic material parameters of the tennis ball, which showed too soft behavior when using the parameters from the material tests.

In this project, the experience of performing explicit FE-calculations and the comprehension of the behavior of an object in a highly dynamic test, have increased. The methods of carrying out dynamic FE-calculations, and to verify them by laboratory testing, have improved. This will give the Division of Mechanics at SP a valuable complement to the real experimental testing in the future.

## REFERENCES

- [1] Hibbit, Karlsson and Sorensen, ABAQUS/Explicit, 1999.
- [2] Recommendations on the Transport of Dangerous Goods, United Nations Publication, 11th edn., 1999.
- [3] EN967:1996, Head protectors for ice hockey players, CEN - European Committee for Standardization, 3rd edn., 1996.
- [4] ISO 37, Rubber, vulcanized or thermoplastic - Determination of tensile stress-strain properties, The International Organization for Standardization, 3rd edn., 1994.